Astro2020 White Paper on Technological Development Activity

On

Wavefront Sensing and Control technologies for Exo-Earth imaging

Authors:

Pueyo Laurent (Space Telescope Science Institute), pueyo@stsci.edu, 410-338-2435
Stark Christopher (Space Telescope Science Institute)

Bailey Vanessa (JPL), Bolcar Matthew (GSFC) Coyle Laura (BATC), Feinberg Lee,(GSFC), Groff Tyler (GSFC), Guyon Olivier (Subaru / Uiversity of Arizona), Jewell Jeffrey (JPL), Kasdin Jeremy (Princeton), Knight Scott (BATC), Mawet Dimitri (Caltech), Mazoyer Johan (JPL), Mennesson Bertrand (JPL), Perrin Marshall (STScI), Redding David (JPL), Riggs AJ (JPL), Ruane Garreth (JPL), Soummer Remi (STScI), Will Scott,(University of Rochester), Zimmerman,Neil,(GSFC)

Summary: This paper focuses on one of the key technologies for high-contrast imaging of potentially Earth-like exoplanets: optical stability through Wavefront Sensing and Control (WFS&C). We briefly review the state of the art in both ground based Extreme Adaptive Optics (ExAO) systems and controlled laboratory experiments dedicated to upcoming space-based missions. Much emphasis is often placed on singular science-related metrics like contrast, while the ability to achieve this contrast over broader bandpasses, a greater range of spatial frequencies, and for a broad range of timescales is just as critical. The latter requires increased WFS&C complexity. As systems have advanced, this additional complexity has been demonstrated and the risk associated with it has been retired. We posit that the maturity of WFS&C technologies is best captured as the *ratio* of demonstrated science capability to architecture risk. We find that the past two decades of combined progress in ExAO and NASA funded experiments has steadily improved the state of the art and we are on track to enable the WFS&C technologies necessary for missions such as HabEx and LUVOIR by $\sim$2025. Even if such technologies have never flown in space, they are well within our reach in the next decade. In order to achieve this milestone we recommend that NASA follows a strategic plan which capitalizes on the combined strengths of ExAO instrumentation and technology testbeds. This will require a cohesive program with dedicated funding lines that foster cross pollination between ground-based instrument builders and NASA technologists. Finally we emphasize the importance of WFIRST-CGI, which has already achieved significant milestones in Phase A, demonstrating for the first time the exquisite performance of an ExAO-like system in a stabilized environment. WFIRST-CGI will be the first demonstration of an ExAO system in space, a key technical milestone in the search for bio-signatures.

1 Key Issue

Decades of exoplanet observations using a variety of techniques have revealed a nearly fantastical universe, filled with exoplanets of an astounding variety. But we have yet to answer, do other Earth-like planets exist? And do they provide an opportunity for life to arise elsewhere? Answering these questions by searching for and characterizing other potentially Earth-like worlds around Sun-like stars is within our grasp for the first time. Indeed, conducting this ambitious experiment is one of the key recommendations of the recent NAS Exoplanet Science Strategy Report [1], and a core focus for two of the four large mission concept studies commissioned by NASA in preparation for Astro2020 [2, 3].

Characterizing potentially Earth-like planets will not be easy. ExoEarths are as faint as some of the faintest extragalactic sources ever detected by Hubble. Spectroscopic exposures to detect potential bio-signatures on these sources will be photon-starved. Even more challenging than extragalactic sources, exoplanets hide in the glare of their host stars, which can be more than ten billion times brighter than the light reflected by the planets. To see these potentially Earth-like planets, we must block the starlight while allowing the planets' light to pass through by using a series of exquisitely optimized optical masks, i.e. a coronagraph.

This paper focuses on one of the key technologies for high contrast coronagraphy: optical stability through Wavefront Sensing and Control (WFS&C). We limit our discussion to stability solutions physically located within the science instrument. Separate white papers by Coyle et al. and Feinberg et al. discuss technologies for optics at the observatory level (telescope, structures, spacecraft). We show that progress over the past decade in dedicated high-contrast testbeds and in Extreme Adaptive Optics (ExAO) instruments has matured WFS&C to a point that is well within reach of what missions like HabEx and LUVOIR need. In order to achieve full readiness by the mid-decade, we recommend that NASA creates funding/programmatic vehicles that enable technologists to capitalize on the remarkable innovation rate of the ExAO community.

2 Technical Overview

Coronagraphs must be designed with the telescope as a system; the geometry of the primary and secondary mirrors, support structures, and segment gaps have a significant impact on performance. Ten years ago, there was not even an adequate *theoretical* solution for coronagraphs with segmented/obscured telescopes. Significant progress has occurred since then [4, 5, 6]. Today's limitations reside in designing coronagraphs that are robust to misalignments and, at the same time, have a sufficiently high throughput when the telescope features a central obscuration (see [7] for details). We now have theoretical coronagraph designs for segmented/obscured apertures that will enable the detection and characterization of Earth-like planets (see white paper by Crill et al). However, these designs will only translate into actual observations *if their optical stability requirements are met.*

2.1 Optical stability and Wavefront Sensing and Control (WFS&C)

To maintain a desired constrast, all coronagraphs require stability over a range of spatial scales. Some of these instabilities are filtered out by the static response of the coronagraph [8, 9] (this is

also called robustness to misalignments), some can be controlled/damped at the observatory level, and others can be allowed to vary, with their impact averaging out. However, all coronagraph designs have a range of pathological misalignment modes to which they are very sensitive. For those modes, to maintain starlight suppression of $\sim 10^{-10}$, pm-level stability must be maintained and controlled as fast as possible. The solution is to introduce Deformable Mirrors (DMs) within the coronagraphic instrument that dynamically adjust to correct wavefront error, along with a wavefront sensing (WFS) system that estimates these errors. Such a system greatly relaxes requirements on the observatory, since pm stability now must only be maintained for the amount of time it takes to sense and correct the wavefront.

Figure 1 shows the flow of light and information for a typical WFS&C system. The observatory level corrections, which we do not discuss here, are shown in the telescope box on the left. Some of the light is separated from the main science beam and reaches WFS&C channel(s), that calculate the wavefront error in real time on board the telescope, and determine the updates to the DMs (and potentially the telescope). While maintaining pm stability during the WFS cycle is challenging, it is not impossible. The LISA pathfinder mission already demonstrated Optical Path Length (OPL) stabilization that is in principle commensurate with stable starlight rejection of $\sim 10^{-10}$. e-LISA's modern passive dampers along with a laser-based metrology system limited the relative acceleration between two test masses, separated by 30 cm, all the way down to $10\ \mathrm{fm\ s^{-2}/sqrt(Hz)}$, over timescales ranging from ten seconds to three hours [10]. At timescales of the order of minutes, these performances can be understood as OPL drifts of about five picometers, remarkably close to what is needed for exoearth imaging in space [11]. Similar measurements have been also carried out for an imaging telescopes in a controlled testbed environment [12], see the whitepaper by Feinberg et al. for more details.

2.2 Ground Based ExAO vs space based WFS&C

Starlight suppression of a few parts in ten billion has already been demonstrated [13] in a controlled testbed environment and with a clear aperture. To date, there has been no end-to-end space-based demonstration of a telescope + coronagraph system that operates at this level of rejection. However, taken independently, the subsystems illustrated on Fig 1 all have a rich history of tests/characterization, either in a laboratory environment, or on-sky with ground-based telescopes, or on orbit. Overall, the challenge associated with coronagraph-based search for life endeavors reside less in the basic technological ingredients, and more in having all of them work together integrated into a complex system with multiple control loops interacting across a range of spatial and temporal scales.

Extreme Adaptive Optics (ExAO). Ground based ExAO instruments routinely take advantage of the architecture in Fig. 1 to yield the image stability necessary to discover young giant planets [14, 15, 16, 17, 18, 19]. Because the spatial and temporal scales of atmospheric turbulence are correlated, achieving image stability close to the star requires correcting a larger number of modes faster [20, 21, 22]. This significantly increases the system complexity associated with ExAO instruments. This push towards faster systems is one of the key drivers underlying exoplanet imaging instrumentations for Extremely Large Telescopes (ELTs). It will bring to full maturity algorithmic advances such as optimal modal decompositions [23] and predictive [24, 25] control and will occur regardless of NASA programmatic decisions. However future missions will greatly benefit from these innovations. Remaining temporal image variations are subtracted using optimized

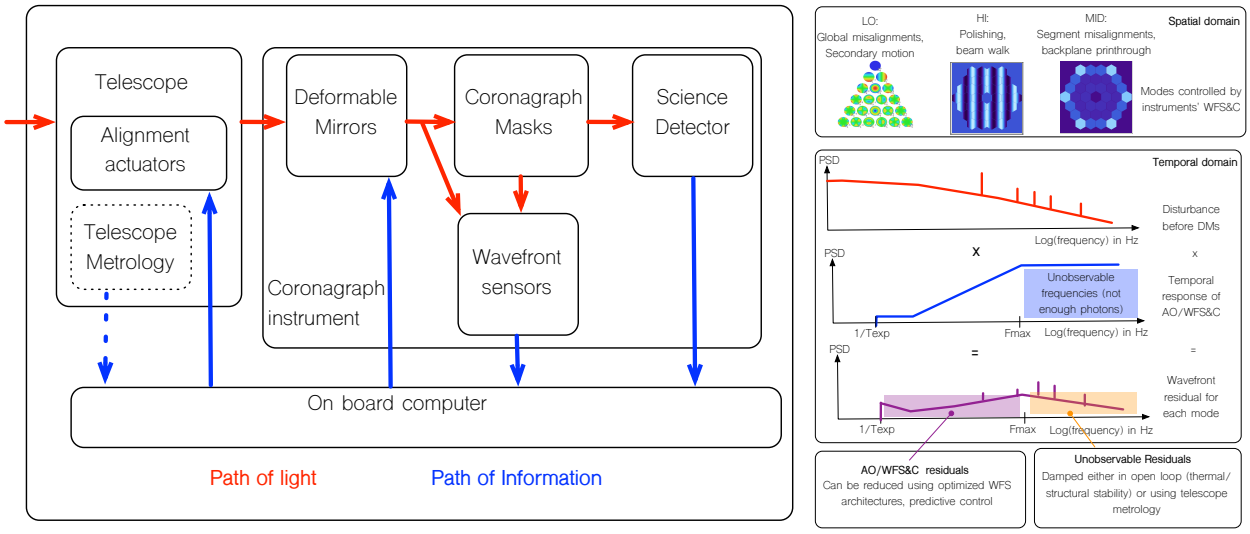

Figure 1: **Left** *Illustration of the main subsystems needed for ExoEarth imaging from space with a coronagraph. Images at the science camera anchor the Deformable Mirrors (DMs) shapes at the $\sim$ cadence of science exposures. For faster variations, auxiliary wavefront sensors provide the information needed for DM updates. This information is fundamentally limited by the numbers of photons received from the exoplanets' host stars.* **Right:** *Representation of the instrument WFS&C response in the frequency domain. Above the cutoff frequency F_{Max}, set by the photon noise, telescope imperfections cannot be corrected by the science instrument. If passive structural damping at the observatory level yields residuals above this frequency, an active metrology system is necessary at the observatory level.*

observation strategies and post-processing algorithms [26, 27, 28], which will also become more sophisticated as ELTs will try to detect planet as close as possible to their host star [29].

Space based coronagraphs. Today's generation of space-based coronagraphs do not feature DMs. Instead, it places a premium on making the environment as stable as possible. HST represents the state or the art, with a stability in a Low Earth Orbit resulting in contrasts at the $\sim 10^{-6}$ level, after post-processing [30]. Models of an improved environment at L2 yields similar performances, at much better resolution and sensitivity, for JWST [31] (albeit at longer wavelengths). WFIRST-CGI simulations predict that a much deeper *static* contrast can be reached once DMs are added [32]. We note that the fundamental coupling between temporal and spatial scales limiting the angular resolution of ground-based observations can be addressed by design for a space-based observatory: engineers can design the thermal and dynamical response of a space telescopes observatory better than they can control the weather. This careful engineering hinges on mechanical and thermal modeling of the observatory (spacecraft+telescope+instruments), which plays a key role in predicting the performances of coronagraphs in space [32, 31]. Such models are extremely complex and have never been fully validated against flight hardware, even at the nanometer level, let alone at the picometer level. Recent JWST cryo-vac thermal tests were a first step towards reconciling observatory integrated models and flight hardware [31]. JWST and WFIRST flight-data will further solidify the fidelity of these models.

ExAO from space. To date, an instrument with auxiliary WFS and DMs has never flown in space. However this is exactly what two of the concepts presented as input to Astro 2020 are proposing, de facto implementing an ExAO system in space (see Fig. 1). Such architectures have been chosen because of the risk/uncertainties associated with open loop wavefront stabilty. Indeed the "set and forget" observing paradigm, hinges on the observatory integrated models to be *exactly* right (at the picometer level), with little room for uncertainty factors. The envisioned closed loop operations flow as follows. The static and very slow errors will be removed by the DMs using diagnostics based on the actual science exposures, as done in [13], using algorithms similar to the ones described in [33, 34, 35]. Note that optical aberrations in the telescope element which change as a function of polarization state, present a particular challenge to achieving deep static contrast [36] because any single set of DM settings can only compensate for the aberrations of one polarization state at a time. Recent simulations, based on the LUVOIR prescription, showed that after DM corrections, residual polarization resulted in a minor deterioration in contrast close to the coronagraph mask and minimal contrast impact elsewhere. Auxiliary wavefront sensors will then provide DM corrections at a cadence faster than the science exposures. The right panel of Fig. 1 illustrates their temporal response (in frequency space). Such technologies, and their operations, have been matured at ground-based observatories, and technology development for future missions needs to optimize them in order to reduce the close loop residual misalignments from the nanometer scale to the picometer scale. As a matter of fact this process is exactly what happened for the WFIRST-CGI instrument: the Zernike WFS was first envisioned and tested for ground based telescopes [37, 38], but quickly adopted and demonstrated in a relevant laboratory environment for WFIRST [39, 40]. Exo-Earth finding missions will have to control more spatial modes than WFIRST, and will require a more optimized WFS architecture. This is where technology transfer between ground based ExAO instruments and space-based missions can be immensely beneficial.

2.3 The importance of WFS architectures

When discussing the feasibility of WFS&C, it is common to focus on the component level, for which there is a major risk associated with successful flight and operations of high density ($1000+$ actuators) DMs technologies capable of repeatable motions at the picometer resolution. Discussing the readiness of such devices is beyond the scope of this paper, and we refer the readers to the discussions in [41, 42, 43] on this topic. Here we assume that the demonstration in [13], combined with future flight projects (either with small satellites [44] or WFIRST-CGI, whitepaper by Bailey et al.) , serves as a robust enough proof of concept as far as DM technologies are concerned.

If the DMs risk is retired, the ultimate performances of WFS&C (or of ExAO) are largely determined at the system level, where the key driver is WFS architecture. Because this sensor is fed with stellar photons, the optimal WFS exposure time is fundamentally set by shot noise from the stellar flux. This results in an upper limit (F_{max}) on the update frequency of the DMs. Under the assumption of perfect components (DMs and detectors) and no control lag, the residual contrast stability also scales with the SNR of the WF estimate. Improving the science performance of an active coronagraphic WFS&C system thus requires estimating the fastest variations possible with sufficient SNR. As a result, an optimal WFS should:

a) receive as many stellar photons as possible. This is achieved by capturing the starlight that is rejected from the coronagraph masks by designing masks as "beamsplitters".

b) minimize the number of optics in the science channel after the WFS pick-off (also called Non-Common Path, NCP). If such optics get misaligned on timescales faster than the science exposure, then the associated image artifacts cannot be sensed and corrected.

c) efficiently convert nanometers of misalignment into intensity variations that can be sensed by a detector. This is quantified using a scalar number, called WFS efficiency that relates WF error and the measurement's photon noise [14, 22].

Table 1 lists some of the WFS architectures in use and being developed today, both for ground- and space-based observatories. The possible architectures for WFSC are many, and the parameter space is vast. They differ significantly in implementation and experimental research in this domain has allowed us to better understand WFS optimization, illustrating the cross-pollination of ground-based ExAO efforts and space-based coronagraph development. The architecture parameter space is too vast to be fully explored and tested in the context of a space mission. It is much more efficient to rapidly prototype and validate using ground-based instrumentation, and then transfer the most promissing architectures to NASA facilities dedicated to technology maturation.

Table 1: Summary of WFS&C technologies demonstrated (either on ground-based telescopes or in dedicated testbeds) over the past decade.

Context	**% of star flux**	**Efficiency**	**NCP optics**	**Notes**
Ground based telescopes				
GPI/SPHERE AO [16, 17]	100	> 2	20+, $\lambda_{Sci} \neq \lambda_{WFS\&C}$	Shack Hartman sensor not sensitive to low order spatial modes. WFS&C $\neq$ science wavelength.
GPI LOWFS [45]	95	> 5	3	Post coronagraph shack Hartman sensor
Mag AO/LBT [46, 47]	100	$\sqrt{2}$	20+, $\lambda_{Sci} \neq \lambda_{WFS\&C}$	Pyramid sensor, loses efficiency when modulated
Focal Plane WFS [48]	10	1	20+	Short exposures in focal plane
Zernike WF [38]	100	1	20+	Cannot be used with coronagraph in the SPHERE implementation
Lyot based WFS [49, 50]	95	1	1	Works with a variety of coronagraphs
Technology testbeds				
LDFC [49, 51]	< 1	1	0	Uses the light outside of the region interest on the science camera
SCC [52]	10	1	1	Turns in the science camera into an interferometer
WFIRST LOWFS, Zernike [39]	95	1	3	Will fly with WFIRST-CGI
Knife Edge WFS [53]	100	1	20+, $\lambda_{Sci} \neq \lambda_{WFS\&C}$	Cannot be used with coronagraph, sensing needs to occur at another wavelength.

2.4 Contrast and complexity as yardsticks of progress

Contrast: The ultimate science performance of coronagraphs is determined by the ability to detect faint planets nearby their host stars. Therefore contrast is commonly used as an expression of the performance of a coronagraph. ExAO coronagraphs are driven by the ability to sense and correct wavefront changes with DMs, and the stability/knowledge of the closed loop residuals. The former scales as raw contrast and the latter as post-processing gain. Because they have no control over the incident disturbance (atmospheric turbulence or drifts in the telescope), ground based systems rely heavily on increasingly sophisticated image analysis algorithms to mitigate the residual noise and find exoplanets. On the other hand, a dedicated space mission operates in a controlled environment in which the incident disturbance can, in principle, be made deterministic. In that context, coronagraphic WFS&C enables larger observatory level drifts (thus reducing observatory complexity)

and mitigates some level of stochasticity in misalignments (decoupling performance from model accuracy, thus reducing risk). Post-processing gains obtained on experiments dedicated to space missions often reflect the environmental stability of a given testbed, that might not be commensurate with projected flight performances. As a result, state of the art in ground based ExAO systems is best captured by the actual flux ratio of detected exoplanets (including post processing) while technology testbeds are best described by their raw contrast.

Table 2: Observations/testbeds considered to derive coronagraph WFS&C nulling efficiency. For ground-based instruments we used properties of actual exoplanets detected as a measure for contrast and separation. For technology testbed we use the raw contrast numbers reported in the literature

Context	**# of Modes**	T_{exp},F_{max}	**Sep** (λ/D)	**Contrast**	**Notes**
Ground based planet discoveries					
2M1207b, 2004 [54]	~ 30	$\sim$ 1hr, 200 Hz	19	5×10^{-3}	No coronagraph, IR WFS&C.
HR8799bcd, 2008 [55]	~ 100	$\sim$ 1hr, 500 Hz	14.5	4×10^{-5}	No coronagraph, Vis WFS&C.
51 Eri b, 2015 [56]	~ 1000	$\sim$ 1hr, 100 Hz	11	2×10^{-6}	No coronagraph, Vis WFS&C.
Technology tesbeds					
JPL, HCIT HLC, 2007 [13]	1	$\sim$ 20hrs, $1/$ (0.9 $\times$ 20hrs)	3	2.5×10^{-10}	One mode corrected at each iteration of EFC [34]. In the absence of mission DRMs timescales of static testbeds are hard to determine. We used the generic 10% overhead along with 20 hrs exposure times [7]
JPL, HCIT Vortex, 2011 [57]	1	$\sim$ 20hrs, $1/$ (0.9 $\times$ 20hrs) Hz	2	1.2×10^{-8}	Same as above
WFIRST-CGI SPC, Static [58]	1	$\sim$ 20hrs, $1/$ (0.9 $\times$ 20hrs) Hz	6.5	7×10^{-9}	Same as above. Early cycles WFIRST-CGI Shaped Pupil Coronagraph (SPC) design.
WFIRST-CGI HLC, Static [58]	1	$\sim$ 20hrs, $1/$ (0.9 $\times$ 20hrs) Hz	3	1.6×10^{-9}	Same as above. Early cycles WFIRST-CGI Hybrid Lyot Coronagraph (HLC) design.
WFIRST-CGI HLC, Dynamic, open loops [59]	1	$\sim$ 20hrs, $1/$ (0.9 $\times$ 20hrs) Hz	3	2×10^{-7}	For this test wavefront variation larger than the testbed environment were injected.
WFIRST-CGI HLC, Dynamic, closed loops [40]	3	$\sim$ 20hrs, 1 Hz	3	7×10^{-9}	For this test wavefront variation larger than the testbed environment were injected and corrected.
WFIRST-CGI SPC, Dynamic, closed loops [40]	3	$\sim$ 20hrs, 1 Hz	4	8×10^{-9}	Same as above.
GSFC, VNC, Static, 2013	200	$\sim$ 3.5hrs, 4 Hz	2	5.5×10^{-9}	Narrowband with no pupil shear. Performed in ambient lab environment.

Instrument complexity: Introducing ExAO-like instrumentation into a space-based observatory mitigates the risk associated with the thermal and mechanical stability of the telescope's large structures. However, the complex WFS&C architectures discussed above also appear as a risky leap forward when compared to ongoing observations with HST. In this context, it is critical to remember that ground-based instruments routinely rely on very similar control systems, albeit at a contrast much shallower than what is needed to image Earth twins. They operate night after night, under the unforgiving thermal gradients of a mountain summit, and still yield misalignment residuals often no larger than a few tens of nanometers (as a reference, the overall JWST wavefront error budget is also a few tens of nanometers). Decades of successes in ExAO instrumentation have already retired a significant fraction of the complexity risk associated with space based WFS&C. We capture this feature by quantifying "how hard" a given instrument or testbed is trying to correct time varying misalignments. We quantify it as the product of the number of independent spatial modes and of the span of timescales corrected (in logarithmic scale).

Ratio of contrast and complexity: We posit a new metric that better reflects progress in the field of coronagraphic WFS&C. When dividing contrast by system complexity for a given instru-

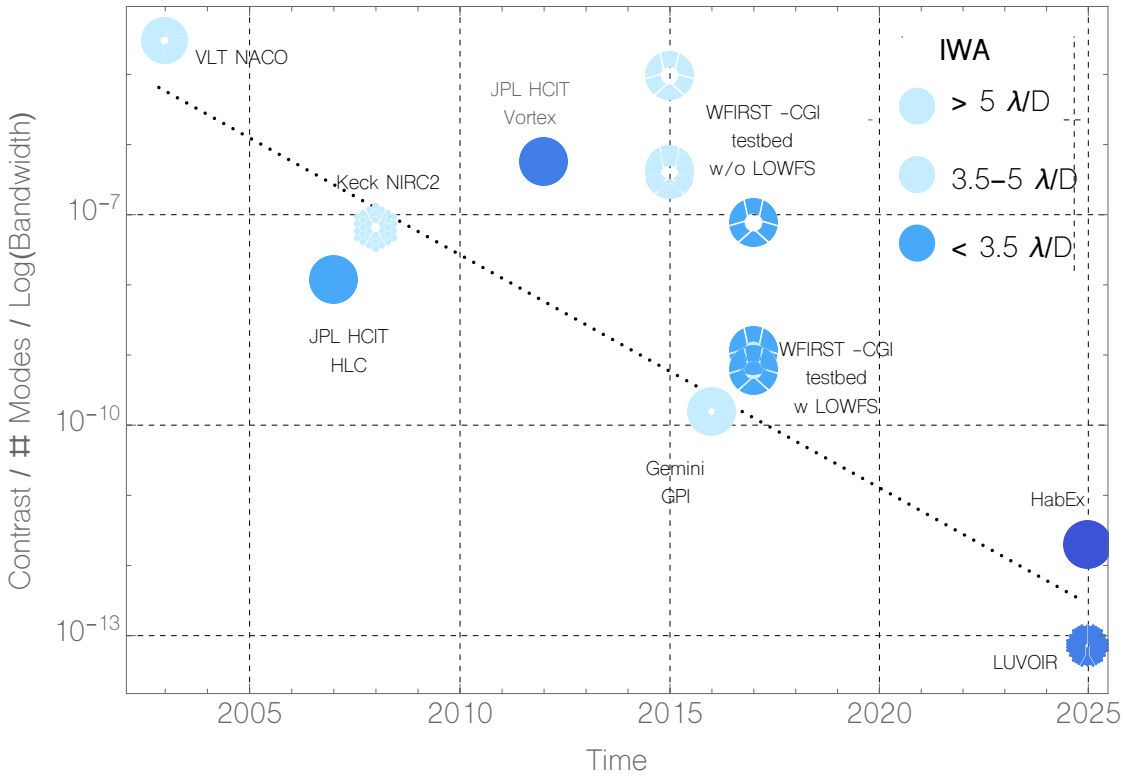

Figure 2: Coronagraph WFS&C modal nulling efficiency as a function of time. The performance has steadily improved over the past two decades. Should progress keep following this pace, coronagraph WFS&C modal nulling efficiency will reach the level required for HabEx or LUVOIR by the mid 2020's.

ment/testbed experiment, one combines demonstrated science performance and retired risk associated with system complexity. We use this ratio to capture the combined state of art of WFS&C in controlled testbeds and ExAO at ground-based telescopes. Note that this ratio is also physically motivated. It scales as the post-coronagraph residual misalignments per corrected mode and per decade of temporal bandwidth. We call this contrast-to-complexity ratio the coronagraph WFS&C modal nulling efficiency.

3 Strategic plan, cost, schedule

3.1 State of the art

Our strategic plan is informed by a review of the state of the art under the light of the considerations discussed above. To do so, we collected the properties of today's ExAO systems and technology testbeds in Table 2 and calculated coronagraph WFS&C modal nulling efficiency for each one of them. Fig. 2 shows how the ratio of science performance and complexity has evolved over time. While the variety of technology testbeds and deployed ExAO systems over the years results in large scatter, the ultimate performance floor under this metric has steadily improved. At first, the

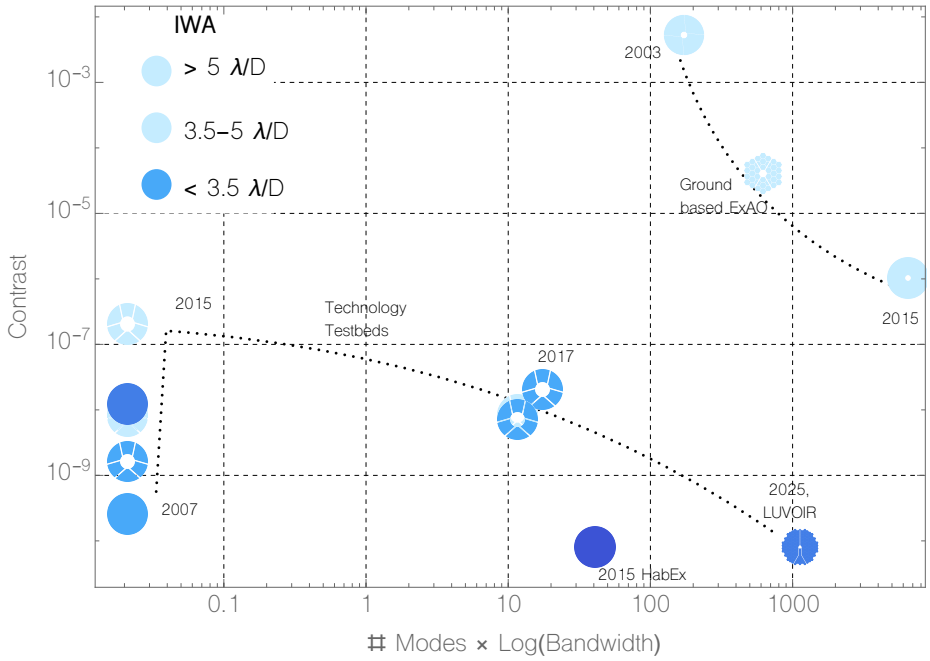

Figure 3: Deconstructing coronagraph modal efficiency: Contrast as a function of system complexity (measured as number of modes per decade of temporal bandpass). While complexity and contrast have steadilty improved for ground based ExAO systems, technogy testbeds focused on very simple WFS&C architectures up until the mid 2010's. Experiments associated with WFIRST-CGI have completely changed this paradigm, they ought to be extended into the next decade.

complexity of instrument based WFS&C necessary for HabEx or LUVOIR seems a paradigm shift when compared to HST or JWST. However, after a closer look at it, Fig. 2 shows that continuing along current progress will result into the required technology demonstration by ∼2025. NASA should aggressively pursue such technologies; they are well within reach in the next decade.

This analysis also reinforces the conclusions of the whitepaper by Crill et al.: the static problem associated with the telescope geometry has been largely solved at the very high level. Indeed, when considering either WFS&C modal nulling efficiency vs time in Fig. 2, or contrast vs WFS&C complexity left panel of Fig. 3, progress does not correlate with aperture complexity. This statement was hard to fathom a decade ago.

3.2 Transfer of ExAO technologies to NASA

In order to reach the coronagraph modal nulling efficiencies required for HabEX or LUVOIR within ∼5 years NASA must articulate a cohesive instrumentation program. This program ought to leverage the strengths of ground based ExAO, and transfer them to space based instrumentation. Motivated by the ELTs, the ground-based ExAO community will continue to innovate and mature accurate and efficient WFS architectures (as indicated on Table 1). Algorithmic advances, ranging from optimal modal decompositions [23] to predictive [24, 25] will be validated on sky and ready

to be pushed to deeper contrasts in the context of ExoEarth imaging. In principle these predictive WFS&C algorithms can greatly relax observatory requirements [60], but are only scarcely used today on space technology testbeds[61, 62, 63]. Such a program would bring these promising algorithms to full maturity. This program would greatly benefit from a small, early investment by NASA to acquire a few dozens of technical nights on 8 meter class telescopes early in the decade.

3.3 Dedicated technology testbed

Dedicated technology testbeds, under a controlled environment, need to demonstrate both the level of contrast required for HabEx or LUVOIR and the system complexity (the relevant range of spatial and temporal scales). The facilities to demonstrate this already exist (summarized in the white paper by Mazoyer et al.). We recommend that the experimental schedule of these testbeds be planned in light or our previous recommendation. Controlled environments are the only platform to reach $\sim 10^{-10}$. Thus, these experiments ought to first focus on what they can do best: validating the theoretical sensitivity (or robustness) of coronagraphs to pathological misalignments. While there now exists a variety of robust designs [8, 9], verifying robustness cannot be done from ground-based telescopes. Such empirical validations are key to extrapolate testbed results to science performances in the formulation phase of any mission. Unfortunately, to the notable exception of recent work on WFIRST-CGI [64], such measurements are often neglected because they are very difficult to carry out [65]. NASA should prioritize the use of existing dedicated technology facilities for such coronagraph model validations. The level of funding for such facilities is currently adequate.

3.4 Funding vehicles for WFS&C technologies

The activities discussed above could either be funded under existing NASA technology calls, or under a dedicated effort. The cost and schedule benefits of such a maturation are argued in the whitepaper by Crooke et al.. To mature technologies for missions like LUVOIR/HabEx by the mid 2020's as suggested, a dedicated funding effort is likely the only feasible option. Distributing the adequate level of funding throughout a number of scattered technology calls is less likely to deliver true paradigm shifting milestones; a cohesive program, such as the one carried out for the coronagraph design and optimization (described in Crill et. al), is much more likely to succeed. Indeed, key historical milestones for WFS&C have typically been achieved in the context of an actual ground-based instrument or a mission in phase A or later; early investments via dedicated programs have enabled these results.

3.5 Continued work WFIRST-CGI

WFIRST-CGI will be the first demonstration of an ExAO system in space, a key milestone in the search for potentially Earth-like planets. Prior to WFIRST-CGI, space technology testbeds did not attempt to add any system complexity to tackle temporal drifts. Driven by milestones associated with WFIRST phase A, the first ExAO-like system was deployed in a stabilized environment and successfully demonstrated at contrasts of $\sim 7 \times 10^{-9}$ [40]. Fig. 3 highlights the important role of this testbed, which for the first time links ground based ExAO systems and technology testbed. It is critical that these investigations continue, and that these results are confirmed on-sky after

WFIRST-CGI launches. Bailey et al. [66] demonstrated how WFIRST-CGI would mature a wide range of technologies—it also plays a critical role in the overall arc of bringing to space complex WFS&C systems, inspired by ground-based instrumentation. In this paper we have argued that this arc is key to the success of the NASA's search of bio-signatures. We thus naturally recommend that the first successful example of such technogy transfer actually gets the opportunity to demonstrate flight readiness and maturity.

References

[1] N. A. of Sciences Engineering and Medicine, *Exoplanet Science Strategy*, The National Academies Press, Washington, DC, 2018.

[2] B. S. Gaudi, S. Seager, B. Mennesson, A. Kiessling, K. Warfield, G. Kuan, K. Cahoy, J. T. Clarke, S. Domagal-Goldman, and L. Feinberg, "The Habitable Exoplanet Observatory (HabEx) Mission Concept Study Interim Report," *arXiv e-prints* , p. arXiv:1809.09674, Sep 2018.

[3] The LUVOIR Team, "The LUVOIR Mission Concept Study Interim Report," *arXiv e-prints* , p. arXiv:1809.09668, Sep 2018.

[4] L. Pueyo and C. Norman, "High-contrast Imaging with an Arbitrary Aperture: Active Compensation of Aperture Discontinuities," *The Astrophysical Journal* **769**, p. 102, June 2013.

[5] O. Guyon, P. M. Hinz, E. Cady, R. Belikov, and F. Martinache, "High Performance Lyot and PIAA Coronagraphy for Arbitrarily Shaped Telescope Apertures," *The Astrophysical Journal* **780**, p. 171, Jan. 2014.

[6] M. N'Diaye, R. Soummer, L. Pueyo, A. Carlotti, C. C. Stark, and M. D. Perrin, "Apodized Pupil Lyot Coronagraphs for Arbitrary Apertures. V. Hybrid Shaped Pupil Designs for Imaging Earth-like planets with Future Space Observatories," *The Astrophysical Journal* **818**, p. 163, Feb. 2016.

[7] S. et al., "Exoearth yield landscape for future direct imaging space telescopes," *Journal of Astronomical Telescopes, Instruments, and Systems* **5**(2), pp. 1 – 20 – 20, 2019.

[8] M. N'Diaye, L. Pueyo, and R. Soummer, "Apodized Pupil Lyot Coronagraphs for Arbitrary Apertures. IV. Reduced Inner Working Angle and Increased Robustness to Low-order Aberrations," *The Astrophysical Journal* **799**, p. 225, Feb. 2015.

[9] G. Ruane, D. Mawet, J. Jewell, and S. Shaklan, "Performance and sensitivity of vortex coronagraphs on segmented space telescopes," *ArXiv e-prints* , Aug. 2017.

[10] M. Armano, H. Audley, J. Baird, P. Binetruy, M. Born, D. Bortoluzzi, E. Castelli, A. Cavalleri, A. Cesarini, A. M. Cruise, K. Danzmann, M. de Deus Silva, I. Diepholz, G. Dixon, R. Dolesi, L. Ferraioli, V. Ferroni, E. D. Fitzsimons, M. Freschi, L. Gesa, F. Gibert, D. Giardini, R. Giusteri, C. Grimani, J. Grzymisch, I. Harrison, G. Heinzel, M. Hewitson, D. Hollington, D. Hoyland, M. Hueller, H. Inchauspé, O. Jennrich, P. Jetzer, N. Karnesis, B. Kaune, N. Korsakova, C. J. Killow, J. A. Lobo, I. Lloro, L. Liu, J. P. López-Zaragoza, R. Maarschalkerweerd, D. Mance, N. Meshksar, V. Martín, L. Martin-Polo, J. Martino, F. Martin-Porqueras, I. Mateos, P. W. McNamara, J. Mendes, L. Mendes, M. Nofrarias, S. Paczkowski, M. Perreur-Lloyd, A. Petiteau, P. Pivato, E. Plagnol, J. Ramos-Castro, J. Reiche, D. I. Robertson, F. Rivas, G. Russano, J. Slutsky, C. F. Sopuerta, T. Sumner, D. Texier, J. I. Thorpe, D. Vetrugno, S. Vitale, G. Wanner, H. Ward, P. J. Wass, W. J. Weber, L. Wissel, A. Wittchen, and P. Zweifel, "Beyond the required lisa free-fall performance: New lisa pathfinder results down to $20\ \mu$Hz," *Phys. Rev. Lett.* **120**, p. 061101, Feb 2018.

[11] B. Nemati, M. T. Stahl, H. P. Stahl, and S. B. Shaklan, "The effects of space telescope primary mirror segment errors on coronagraph instrument performance," in *Society of Photo-Optical Instrumentation Engineers (SPIE) Conference Series*, *Society of Photo-Optical Instrumentation Engineers (SPIE) Conference Series* **10398**, p. 103980G, Sep 2017.

[12] B. Saif, P. Greenfield, M. North-Morris, M. Bluth, L. Feinberg, J. C. Wyant, and R. Keski-Kuha, "Sub-picometer dynamic measurements of a diffuse surface," **58**, p. 3156, Apr 2019.

[13] J. T. Trauger and W. A. Traub, "A laboratory demonstration of the capability to image an Earth-like extrasolar planet," *Nature* **446**, pp. 771–773, Apr. 2007.

[14] O. Guyon, "Limits of Adaptive Optics for High-Contrast Imaging," *The Astrophysical Journal* **629**, pp. 592–614, Aug. 2005.

[15] T. Fusco, C. Petit, G. Rousset, J.-F. Sauvage, K. Dohlen, D. Mouillet, J. Charton, P. Baudoz, M. Kasper, E. Fedrigo, P. Rabou, P. Feautrier, M. Downing, P. Gigan, J.-M. Conan, J.-L. Beuzit, N. Hubin, F. Wildi, and P. Puget, "Design of the extreme AO system for SPHERE, the planet finder instrument of the VLT," in *Proceedings of the SPIE*, *Proceedings of the SPIE* **6272**, p. 17, July 2006.

[16] L. A. Poyneer, R. J. De Rosa, B. Macintosh, D. W. Palmer, M. D. Perrin, N. Sadakuni, D. Savransky, B. Bauman, A. Cardwell, and J. K. Chilcote, "On-sky performance during verification and commissioning of the Gemini Planet Imager's adaptive optics system," in *Adaptive Optics Systems IV*, *Society of Photo-Optical Instrumentation Engineers (SPIE) Conference Series* **9148**, p. 91480K, Jul 2014.

[17] T. Fusco, J. F. Sauvage, D. Mouillet, A. Costille, C. Petit, J. L. Beuzit, K. Dohlen, J. Milli, J. Girard, and M. Kasper, "SAXO, the SPHERE extreme AO system: on-sky final performance and future improvements," in *Adaptive Optics Systems V*, *Society of Photo-Optical Instrumentation Engineers (SPIE) Conference Series* **9909**, p. 99090U, Jul 2016.

[18] J. Lozi, O. Guyon, N. Jovanovic, N. Takato, G. Singh, B. Norris, H. Okita, T. Bando, and F. Martinache, "Characterizing Vibrations at the Subaru Telescope for the Subaru Coronagraphic Extreme Adaptive Optics instrument," *arXiv e-prints* , p. arXiv:1809.08296, Sep 2018.

[19] O. Guyon, "Extreme adaptive optics," *Annual Review of Astronomy and Astrophysics* **56**(1), pp. 315–355, 2018.

[20] D. Mawet, L. Pueyo, P. Lawson, L. Mugnier, W. Traub, A. Boccaletti, J. T. Trauger, S. Gladysz, E. Serabyn, J. Milli, R. Belikov, M. Kasper, P. Baudoz, B. Macintosh, C. Marois, B. Oppenheimer, H. Barrett, J.-L. Beuzit, N. Devaney, J. Girard, O. Guyon, J. Krist, B. Mennesson, D. Mouillet, N. Murakami, L. Poyneer, D. Savransky, C. Vérinaud, and J. K. Wallace, "Review of small-angle coronagraphic techniques in the wake of ground-based second-generation adaptive optics systems," in *Proceedings of the SPIE*, *Proceedings of the SPIE* **8442**, p. 04, (eprint: arXiv:1207.5481), Sept. 2012.

[21] J. R. Males, L. M. Close, K. Miller, L. Schatz, D. Doelman, J. Lumbres, F. Snik, A. Rodack, J. Knight, and K. Van Gorkom, "MagAO-X: project status and first laboratory results," in *Adaptive Optics Systems VI*, *Society of Photo-Optical Instrumentation Engineers (SPIE) Conference Series* **10703**, p. 1070309, Jul 2018.

[22] O. Guyon, "Extreme Adaptive Optics," *Annual Review of Astronomy and Astrophysics* **56**, pp. 315–355, Sep 2018.

[23] O. Guyon and J. Males, "Adaptive Optics Predictive Control with Empirical Orthogonal Functions (EOFs)," *arXiv e-prints* , p. arXiv:1707.00570, Jul 2017.

[24] L. A. Poyneer and J.-P. Véran, "Optimal modal Fourier-transform wavefront control," *Journal of the Optical Society of America A* **22**, pp. 1515–1526, Aug. 2005.

[25] O. G. Jared R. Males, "Ground-based adaptive optics coronagraphic performance under closed-loop predictive control," *Journal of Astronomical Telescopes, Instruments, and Systems* **4**(1), pp. 1 – 21 – 21, 2018.

[26] C. Marois, D. Lafrenière, R. Doyon, B. Macintosh, and D. Nadeau, "Angular Differential Imaging: A Powerful High-Contrast Imaging Technique," *The Astrophysical Journal* **641**, p. 556, Apr. 2006.

[27] D. Lafreniere, C. Marois, R. Doyon, D. Nadeau, and É. Artigau, "A new algorithm for point-spread function subtraction in high-contrast imaging: A demonstration with angular differential imaging," *The Astrophysical Journal* **660**(1), p. 770, 2007.

[28] R. Soummer, L. Pueyo, and J. Larkin, "Detection and Characterization of Exoplanets and Disks Using Projections on Karhunen-Loève Eigenimages," *The Astrophysical Journal Letters* **755**, p. L28, Aug. 2012.

[29] N. Jovanovic, O. Absil, P. Baudoz, M. Beaulieu, M. Bottom, E. Cady, B. Carlomagno, A. Carlotti, D. Doelman, and K. Fogarty, "Review of high-contrast imaging systems for current and future ground-based and space-based telescopes: Part II. Common path wavefront sensing/control and coherent differential imaging," in , *Society of Photo-Optical Instrumentation Engineers (SPIE) Conference Series* **10703**, p. 107031U, Jul 2018.

[30] J. H. Debes, B. Ren, and G. Schneider, "Pushing the Limits of the Coronagraphic Occulters on HST/STIS," *arXiv e-prints* , p. arXiv:1905.06838, May 2019.

[31] M. D. Perrin, L. Pueyo, K. Van Gorkom, K. Brooks, A. Rajan, J. Girard, and C.-P. Lajoie, "Updated optical modeling of jwst coronagraph performance contrast, stability, and strategies," 2018.

[32] J. Krist, B. Nemati, and B. Mennesson, "Numerical modeling of the proposed WFIRST-AFTA coronagraphs and their predicted performances," *Journal of Astronomical Telescopes, Instruments, and Systems* **2**, p. 011003, Jan. 2016.

[33] P. J. Bordé and W. A. Traub, "High-Contrast Imaging from Space: Speckle Nulling in a Low-Aberration Regime," *The Astrophysical Journal* **638**, p. 488, Feb. 2006.

[34] A. Give'on, B. Kern, S. Shaklan, D. C. Moody, and L. Pueyo, "Broadband wavefront correction algorithm for high-contrast imaging systems," in *Proceedings of the SPIE*, *Proceedings of the SPIE* **6691**, p. 66910A, Sept. 2007.

[35] L. Pueyo, J. Kay, N. J. Kasdin, T. Groff, M. McElwain, A. Give'on, and R. Belikov, "Optimal dark hole generation via two deformable mirrors with stroke minimization," *Applied Optics* **48**, p. 6296, Nov. 2009.

[36] J. B. Breckinridge and R. A. Chipman, "Telescope polarization and image quality: Lyot coronagraph performance," in , *Society of Photo-Optical Instrumentation Engineers (SPIE) Conference Series* **9904**, p. 99041C, Jul 2016.

[37] M. N'Diaye, K. Dohlen, T. Fusco, and B. Paul, "Calibration of quasi-static aberrations in exoplanet direct-imaging instruments with a Zernike phase-mask sensor," *Astronomy and Astrophysics* **555**, p. A94, July 2013.

[38] M. N'Diaye, A. Vigan, K. Dohlen, J. F. Sauvage, A. Caillat, A. Costille, J. H. V. Girard, J. L. Beuzit, T. Fusco, and P. Blanchard, "Calibration of quasi-static aberrations in exoplanet direct-imaging instruments with a Zernike phase-mask sensor. II. Concept validation with ZELDA on VLT/SPHERE," **592**, p. A79, Aug 2016.

[39] F. Shi, K. Balasubramanian, R. Bartos, R. Hein, R. Lam, M. Mandic, D. Moore, J. Moore, K. Patterson, I. Poberezhskiy, J. Shields, E. Sidick, H. Tang, T. Truong, J. K. Wallace, X. Wang, and D. W. Wilson, "Low order wavefront sensing and control for WFIRST coronagraph," in *Space Telescopes and Instrumentation 2016: Optical, Infrared, and Millimeter Wave*, *Procs SPIE* **9904**, p. 990418, July 2016.

[40] F. Shi, E. Cady, B.-J. Seo, X. An, K. Balasubramanian, B. Kern, R. Lam, D. Marx, D. Moody, and C. Mejia Prada, "Dynamic testbed demonstration of WFIRST coronagraph low order wavefront sensing and control (LOWFS/C)," in *Procs SPIE*, *Society of Photo-Optical Instrumentation Engineers (SPIE) Conference Series* **10400**, p. 104000D, Sep 2017.

[41] P. Y. Madec, "Overview of deformable mirror technologies for adaptive optics and astronomy," in *Procs SPIE*, *Society of Photo-Optical Instrumentation Engineers (SPIE) Conference Series* **8447**, p. 844705, Jul 2012.

[42] A. Wirth, J. Cavaco, T. Bruno, and K. M. Ezzo, "Deformable mirror technologies at aoa xinetics," 2013.

[43] R. E. Morgan, E. S. Douglas, G. W. Allan, P. Bierden, S. Chakrabarti, T. Cook, M. Egan, G. Furesz, J. N. Gubner, T. D. Groff, C. A. Haughwout, B. G. Holden, C. B. Mendillo, M. Ouellet, P. do Vale Pereira, A. J. Stein, S. Thibault, X. Wu, Y. Xin, and K. L. Cahoy, "Mems deformable mirrors for space-based high-contrast imaging," *Micromachines* **10**(6), 2019.

[44] G. Allan, E. S. Douglas, D. Barnes, M. Egan, G. Furesz, W. Grunwald, J. Gubner, C. Haughwout, B. G. Holden, and P. do Vale Pereira, "The deformable mirror demonstration mission (DeMi) CubeSat: optomechanical design validation and laboratory calibration," in , *Society*

of Photo-Optical Instrumentation Engineers (SPIE) Conference Series **10698**, p. 1069857, Aug 2018.

[45] J. K. Wallace, J. Angione, R. Bartos, P. Best, R. Burruss, F. Fregoso, B. M. Levine, B. Nemati, M. Shao, and C. Shelton, "Post-coronagraph wavefront sensor for Gemini Planet Imager," in *Proceedings of the SPIE*, *Proceedings of the SPIE* **7015**, p. 70156N, July 2008.

[46] V. P. Bailey, P. M. Hinz, A. T. Puglisi, S. Esposito, V. Vaitheeswaran, A. J. Skemer, D. Defrère, A. Vaz, and J. M. Leisenring, "Large binocular telescope interferometer adaptive optics: on-sky performance and lessons learned," in *Procs SPIE*, *Society of Photo-Optical Instrumentation Engineers (SPIE) Conference Series* **9148**, p. 914803, Jul 2014.

[47] L. M. Close, J. R. Males, K. M. Morzinski, S. Esposito, A. Riccardi, R. Briguglio, K. B. Follette, Y.-L. Wu, E. Pinna, and A. Puglisi, "Status of MagAO and review of astronomical science with visible light adaptive optics," in *Procs SPIE*, *Society of Photo-Optical Instrumentation Engineers (SPIE) Conference Series* **10703**, p. 107030L, Jul 2018.

[48] M. N'Diaye, F. Martinache, N. Jovanovic, J. Lozi, O. Guyon, B. Norris, A. Ceau, and D. Mary, "Calibration of the island effect: Experimental validation of closed-loop focal plane wavefront control on Subaru/SCExAO," *A&A* **610**, p. A18, Feb 2018.

[49] G. Singh, J. Lozi, O. Guyon, P. Baudoz, N. Jovanovic, F. Martinache, T. Kudo, E. Serabyn, and J. Kuhn, "On-Sky Demonstration of Low-Order Wavefront Sensing and Control with Focal Plane Phase Mask Coronagraphs," *PASP* **127**, p. 857, Sep 2015.

[50] G. Singh, J. Lozi, N. Jovanovic, O. Guyon, P. Baudoz, F. Martinache, and T. Kudo, "A Demonstration of a Versatile Low-order Wavefront Sensor Tested on Multiple Coronographs," *PASP* **129**, p. 095002, Sep 2017.

[51] K. Miller, O. Guyon, and J. Males, "Spatial linear dark field control: stabilizing deep contrast for exoplanet imaging using bright speckles," *Journal of Astronomical Telescopes, Instruments, and Systems* **3**, p. 049002, Oct 2017.

[52] J. Mazoyer, P. Baudoz, R. Galicher, M. Mas, and G. Rousset, "Estimation and correction of wavefront aberrations using the self-coherent camera: laboratory results," *A&A* **557**, p. A9, Sep 2013.

[53] S. K. Zareh, J. K. Wallace, F. Loya, and D. Redding, "A simple, dual knife-edge test for phasing segmented aperture space telescopes," in *Procs SPIE*, *Society of Photo-Optical Instrumentation Engineers (SPIE) Conference Series* **10706**, p. 107064Q, Jul 2018.

[54] G. Chauvin, A.-M. Lagrange, C. Dumas, B. Zuckerman, D. Mouillet, I. Song, J.-L. Beuzit, and P. Lowrance, "A giant planet candidate near a young brown dwarf. Direct VLT/NACO observations using IR wavefront sensing," *Astronomy and Astrophysics* **425**, pp. L29–L32, Oct. 2004.

[55] C. Marois, B. Macintosh, T. Barman, B. Zuckerman, I. Song, J. Patience, D. Lafrenière, and R. Doyon, "Direct Imaging of Multiple Planets Orbiting the Star HR 8799," *Science* **322**, pp. 1348–1352, Nov. 2008.

[56] B. Macintosh, J. R. Graham, T. Barman, R. J. De Rosa, Q. Konopacky, M. S. Marley, C. Marois, E. L. Nielsen, L. Pueyo, A. Rajan, J. Rameau, D. Saumon, J. J. Wang, J. Patience, M. Ammons, P. Arriaga, E. Artigau, S. Beckwith, J. Brewster, S. Bruzzone, J. Bulger, B. Burningham, A. S. Burrows, C. Chen, E. Chiang, J. K. Chilcote, R. I. Dawson, R. Dong, R. Doyon, Z. H. Draper, G. Duchêne, T. M. Esposito, D. Fabrycky, M. P. Fitzgerald, K. B. Follette, J. J. Fortney, B. Gerard, S. Goodsell, A. Z. Greenbaum, P. Hibon, S. Hinkley, T. H. Cotten, L.-W. Hung, P. Ingraham, M. Johnson-Groh, P. Kalas, D. Lafreniere, J. E. Larkin, J. Lee, M. Line, D. Long, J. Maire, F. Marchis, B. C. Matthews, C. E. Max, S. Metchev, M. A. Millar-Blanchaer, T. Mittal, C. V. Morley, K. M. Morzinski, R. Murray-Clay, R. Oppenheimer, D. W. Palmer, R. Patel, M. D. Perrin, L. A. Poyneer, R. R. Rafikov, F. T. Rantakyrö, E. L. Rice, P. Rojo, A. R. Rudy, J.-B. Ruffio, M. T. Ruiz, N. Sadakuni, L. Saddlemyer, M. Salama, D. Savransky, A. C. Schneider, A. Sivaramakrishnan, I. Song, R. Soummer, S. Thomas, G. Vasisht, J. K. Wallace, K. Ward-Duong, S. J. Wiktorowicz, S. G. Wolff, and B. Zuckerman, "Discovery and spectroscopy of the young jovian planet 51 Eri b with the Gemini Planet Imager," *Science* **350**, pp. 64–67, Oct. 2015.

[57] D. Mawet, E. Serabyn, D. Moody, B. Kern, A. Niessner, A. Kuhnert, D. Shemo, R. Chipman, S. McClain, and J. Trauger, "Recent results of the second generation of vector vortex coronagraphs on the high-contrast imaging testbed at JPL," in *Proceedings of the SPIE*, *Proceedings of the SPIE* **8151**, p. 81511D, Oct. 2011.

[58] E. Cady, C. Mejia Prada, X. An, K. Balasubramanian, R. Diaz, N. J. Kasdin, B. Kern, A. Kuhnert, B. Nemati, and K. Patterson, "Laboratory performance of the shaped pupil coronagraphic architecture for the WFIRST/AFTA coronagraph," in *Procs SPIE*, *Society of Photo-Optical Instrumentation Engineers (SPIE) Conference Series* **9605**, p. 96050B, Sep 2015.

[59] B.-J. Seo, E. Cady, B. Gordon, B. Kern, R. Lam, D. Marx, D. Moody, R. Muller, K. Patterson, and I. Poberezhskiy, "Hybrid Lyot coronagraph for WFIRST: high-contrast broadband testbed demonstration," in *Procs SPIE*, *Society of Photo-Optical Instrumentation Engineers (SPIE) Conference Series* **10400**, p. 104000F, Sep 2017.

[60] L. Pogorelyuk and N. J. Kasdin, "Dark Hole Maintenance and A Posteriori Intensity Estimation in the Presence of Speckle Drift in a High-contrast Space Coronagraph," *ApJ* **873**, p. 95, Mar 2019.

[61] T. D. Groff and N. Jeremy Kasdin, "Kalman filtering techniques for focal plane electric field estimation," *Journal of the Optical Society of America A* **30**, p. 128, Jan. 2013.

[62] A. J. E. Riggs, N. J. Kasdin, and T. D. Groff, "Wavefront correction with Kalman filtering for the WFIRST-AFTA coronagraph instrument," in *Proceedings of the SPIE*, *Proceedings of the SPIE* **9605**, p. 960507, Sept. 2015.

[63] A. J. E. Riggs, N. J. Kasdin, and T. D. Groff, "Recursive starlight and bias estimation for high-contrast imaging with an extended Kalman filter," *Journal of Astronomical Telescopes, Instruments, and Systems* **2**, p. 011017, Jan. 2016.

[64] H. Zhou, J. Krist, E. Cady, and I. Poberezhskiy, "High accuracy coronagraph flight WFC model for WFIRST-CGI raw contrast sensitivity analysis," in *Procs SPIE*, *Society of Photo-Optical Instrumentation Engineers (SPIE) Conference Series* **10698**, p. 106982M, Jul 2018.

[65] E. Sidick, S. Shaklan, A. Give'on, and B. Kern, "Studies of the effects of optical system errors on the HCIT contrast performance," in , *Society of Photo-Optical Instrumentation Engineers (SPIE) Conference Series* **8151**, p. 815106, Oct 2011.

[66] V. P. Bailey, L. Armus, B. Balasubramanian, P. Baudoz, A. Bellini, D. Benford, B. Berriman, A. Bhattacharya, A. Boccaletti, and E. Cady, "Key Technologies for the Wide Field Infrared Survey Telescope Coronagraph Instrument," *arXiv e-prints* , p. arXiv:1901.04050, Jan 2019.